



Published in final edited form as:

*Clin Breast Cancer*. 2017 February ; 17(1): e11–e18. doi:10.1016/j.clbc.2016.07.009.

## Invasive Breast Cancer Preferably and Predominantly Occurs at the Interface between Fibroglandular and Adipose Tissue

Wenlian Zhu<sup>1</sup>, Susan Harvey<sup>2</sup>, Katarzyna J. Macura<sup>2,3</sup>, David M. Euhus<sup>3,4</sup>, and Dmitri Artemov<sup>1,3</sup>

<sup>1</sup>Division of Cancer Imaging Research, Russell H. Morgan Department of Radiology and Radiological Sciences, Johns Hopkins University School of Medicine, Baltimore, Maryland 21205, USA

<sup>2</sup>Russell H. Morgan Department of Radiology and Radiological Sciences, Johns Hopkins University School of Medicine, Baltimore, Maryland 21205, USA

<sup>3</sup>Sidney Kimmel Comprehensive Cancer Center, Johns Hopkins University School of Medicine, Baltimore, Maryland 21205, USA

<sup>4</sup>Department of Surgery, Johns Hopkins University School of Medicine, Baltimore, Maryland 21205, USA

### Abstract

**Background**—Increasing evidence suggests adipocyte involvement in malignant breast tumor invasive front or margin. The aim of this study was to evaluate the location of invasive breast tumors in relation to the fibroglandular and adipose tissue, using DCE-MRI images.

**Patients and Methods**—Pre-treatment breast DCE-MRI images of 294 patients with biopsy-proven invasive breast cancer from 2008 to 2014 were studied. Invasive breast tumors were visualized as enhanced lesions in the post-contrast subtraction images. Positive identification of the biopsy-confirmed invasive breast tumors on DCE-MRI images was achieved by correlation of findings from breast MRI and pathology reports. Tumor location in relation to fibroglandular and adipose tissue was investigated using pre-contrast T<sub>1</sub>-weighted MRI images.

**Results**—Of 294 patients, 291 had DCE-MRI discernable invasive breast tumors located at the interface between fibroglandular and adipose tissues, regardless of the tumor size, type, receptor status, or breast composition.

**Conclusion**—Invasive breast cancer preferably and predominantly occurs adjacent to breast adipose tissue.

### Micro Abstract

The position of invasive breast tumor in relation to fibroglandular and adipose tissue was assessed in this retrospective DCE-MRI investigation of 294 patients. These tumors were found to occur predominantly at the interface between fibroglandular and adipose tissue.

---

Correspondence: Wenlian Zhu, PhD, Phone: 443-287-4426, Fax: 410-614-1948, wzhu3@jhmi.edu.

#### Disclosure

The authors have stated that they have no conflict of interest.

## Keywords

breast cancer; MRI; adipose; fibroglandular; involution

---

## Introduction

The human breast is composed mainly of fibroglandular and adipose tissue. Although breast carcinoma is a type of cancer that arises from the epithelial cells that line the lobules and terminal ducts of breast glandular tissue<sup>1</sup>, it develops in a complex tissue environment and depends on bidirectional communication with other tissues for tumor initiation and progression<sup>2</sup>. Adipose tissue is of special interest because it is one of the major components in the breast. Increasing evidence suggests adipocyte involvement in the breast tumor invasive front or margin, presumably due to the close proximity of adipose and glandular tissue<sup>3</sup>. An earlier histology study of 310 patients with invasive ductal carcinoma of the breast demonstrated that adipose tissue was present in the breast tumor margin of 245 patients<sup>4</sup>. While some studies have reported cross-talk between breast tumor cells and peritumoral adipocytes<sup>5, 6</sup>, it is not known whether this cross-talk is incidental or obligatory in breast cancer initiation and development. The investigation into the breast tumor microenvironment has mainly been focused on non-adipocyte components<sup>7</sup>.

Overall adiposity plays an important role in many epithelial malignancies, including breast cancer, as manifested by increased breast cancer incidence rates in overweight/obese women<sup>8-10</sup>. Obesity is associated with systemic effects, including insulin resistance, altered hormone signaling, and high circulating levels of proinflammatory mediators that favor tumor initiation and progression<sup>11-13</sup>. However, the local effect of adipocytes in breast cancer has been less explored. In addition, the breast is a unique and dynamic organ. Breast density, a measurement of the fibroglandular/adipose tissue composition, fluctuates throughout an adult woman's life due to factors such as weight gain, pregnancy, lactation, and mammary- and age-related lobular involution. There has been a longstanding interest in the relationship between breast cancer and involution<sup>14-18</sup>, during which breast fibroglandular tissue is replaced by adipose tissue.

We aimed to evaluate the location of invasive breast tumors in relation to fibroglandular and adipose tissue, using DCE-MRI images in this retrospective study. DCE-MRI is an ideal tool with which to investigate the macroscopic interaction between adipose tissue and breast tumors. Malignant breast tumors are identified on post-contrast subtraction images by a rapid enhancement due to their increased vascularity, while adipose and fibroglandular tissue can be differentiated in the corresponding pre-contrast T<sub>1</sub>-weighted images.

## Methods

### Patient Selection

This retrospective DCE-MRI study of invasive breast cancer patients was approved by our Institutional Review Board under the Health Insurance Portability and Accountability Act. The requirement for consent was waived. Breast MRI images and reports acquired from

October 2008 to December 2014 at our Outpatient Center were reviewed consecutively using the picture archiving and communication system (PACS) database. Those with a biopsy-proven unilateral invasive breast cancer diagnosis or suspicious lesions were identified from the MRI reports. These patients' electronic medical records were subsequently reviewed to confirm the presence of an invasive breast cancer diagnosis. Only those who had an MRI performed before any breast cancer related therapeutic intervention were included in the current study. Women with a prior history of breast surgery and/or cancer of any organs were excluded. This study was limited to invasive breast cancer only. Women with a diagnosis of ductal carcinoma in situ were also excluded.

### **Breast DCE-MRI Image Acquisition Techniques**

Clinical breast DCE-MRI acquisition techniques have evolved over the years in our institution. Early images were acquired with relatively thicker slices and without fat saturation in order to achieve a high temporal resolution. New techniques that allowed thinner slices with fat saturation were gradually adapted after 2014.

Three-dimensional, axial, DCE-MRI images without fat saturation that covered both breasts entirely were acquired with the following parameters: TR/TE, 4.2/2.1 ms; flip angle, 10°; slice thickness, 2.5 – 2.7 mm; and in-plane resolution of 0.33 mm × 0.33 mm to 0.67 mm × 0.67 mm at a temporal resolution of 15 sec/acquisition. Gadobenate dimeglumine (Multihance, Bracco Imaging) was administered intravenously at a dose of 0.1 mmol/kg and an injection rate of 2 mL/s, using a power injector (Spectris Solaris MR Injection System, Medrad). DCE-MRI was performed on one of the 1.5-T Achieva (Philips Medical System, Andover, MA), 3-T Intera (Philips Medical System, Andover, MA), or 3-T TrioTim (Siemens, Erlangen, Germany) MRI scanners, using bilateral, phased-array breast coils with patients lying in the prone position.

Three-dimensional axial DCE-MRI images with fat saturation that covered both breasts entirely were acquired with the following parameters: TR 4.9 – 7.8 ms, TE 2.5 – 4.8 ms; flip angle, 12°; slice thickness, 0.5 – 1.5 mm; and in-plane resolution 0.66 mm × 0.66 mm to 0.91 mm × 0.91 mm at a temporal resolution of 16 – 93 sec/acquisition on the 3-T Intera (Philips Medical System, Andover, MA), or 3-T TrioTim (Siemens, Erlangen, Germany) MRI scanners, using bilateral, phased-array breast coils with patients lying in the prone position. Gadobenate dimeglumine (Multihance, Bracco Imaging) was administered intravenously at a dose of 0.1 mmol/kg and an injection rate of 2 mL/s, using a power injector (Spectris Solaris MR Injection System, Medrad).

### **Breast Tumor Identification**

Enhanced breast lesions were visually identified on the post-contrast subtraction images after the contrast enhancement reached a plateau, which occurred about 1 – 2 minutes after the administration of the contrast agent. Findings from the official breast MRI reports and pathology reports were used to confirm whether these enhanced lesions were indeed the pathology-proven invasive breast tumors.

### Location of the Breast Tumor in Relation to Adipose Tissue

Breast fibroglandular and adipose tissues were differentiated by their strong intensity difference on the pre-contrast T<sub>1</sub>-weighted images. Adipose tissue appeared bright and fibroglandular appeared dark on the T<sub>1</sub>-weighted images without fat saturation. The contrast between adipose and fibroglandular tissue is reversed on T<sub>1</sub>-weighted images with fat saturation. The breast tumor position in relation to adipose tissue was visually assessed by overlaying the contrast-enhanced MRI images on the corresponding T<sub>1</sub>-weighted pre-contrast images. Image analysis and visualization were performed in Fiji/ImageJ<sup>19, 20</sup>.

### Breast Density Assessment and the Thickness of the Upper Abdominal Adipose Layer

Three-dimensional MRI breast density was calculated from the contralateral breast with no tumor from the pre-contrast T<sub>1</sub>-weighted images without fat saturation as described<sup>21</sup>. Briefly, bright fatty tissue and the entire breast were segmented by thresholding separately after the correction of image intensity bias artifacts due to magnetic field heterogeneity. Total voxel counts of the fatty tissue and the entire breast were calculated by an automated macro. Percent fatty tissue density was calculated as the percentage of total voxel counts occupied by the fatty tissues divided by that of the entire breast. The MRI percent breast density was calculated as the remaining percentage of the fatty tissue<sup>21</sup>.

The thickness of the upper abdominal adipose layer (UAAL) was measured on the T<sub>1</sub>-weighted pre-contrast axial images immediately below the breasts. This thickness was used as a surrogate marker for body adiposity due to a lack of body mass index information in this retrospective study<sup>21</sup>.

## Results

### Patient Selection Characteristics

Breast DCE-MRI was performed in our institution for high-risk screening<sup>22</sup>, evaluation of a suspicious lesion/lump, and treatment planning following a breast cancer diagnosis, all at the discretion of treating physicians. A total of 294 consecutive patients diagnosed with unilateral invasive breast cancer with pre-treatment breast DCE-MRI performed from October 2008 to December 2014 in our outpatient center were identified by MRI reports and the corresponding medical records. MRI breast density measurements for these patients have been previously reported<sup>21</sup>. The indication for breast DCE-MRI was for the evaluation of disease extent and treatment planning following a biopsy-proven invasive breast cancer diagnosis for a majority of these patients (276, 94%). Fifteen of the 294 patients had DCE-MRI performed to evaluate suspicious breast lesions/lumps or bloody discharge and were subsequently diagnosed with invasive breast cancer. The remaining two patients were diagnosed with invasive breast cancer during their routine high-risk DCE-MRI screening.

Breast DCE-MRI was performed without fat saturation in 278 patients and with fat saturation in 16 patients.

### **Patient Age, Body Adiposity, and Breast Density**

The age of these patients ranged from 25 to 80 years. The thickness of the UAAL, a surrogate marker for body adiposity, ranged from 1 to 37 mm. The MRI breast density of these patients was calculated from the T<sub>1</sub>-weighted pre-contrast images, as described earlier<sup>21</sup>. The density ranged from very dense at 80.7% to very fatty at 3.2%. Patient age, the thickness of the UAAL, and MRI breast density distribution are listed in Table 1.

### **Breast Cancer Receptor Status**

Immunohistochemistry studies indicated that 69.4% of these tumors were estrogen and/or progesterone receptor-positive, 5.4% were HER-2 receptor-positive only, 13.6% were estrogen- and/or progesterone-positive and HER-2 receptor-positive, and 11.2% were triple-negative (estrogen and progesterone receptor-negative, and HER-2 receptor-negative)<sup>23</sup>. Receptor status was not available in the medical records for one patient.

### **Breast Cancer Stage**

Pathologic tumor stage was available in 224(76.2%) patients who received adjuvant therapy with the following results: 148 patients at stage 1; 67 patients at stage 2; 8 patients at stage 3; and 1 patient at stage 4<sup>24</sup>. Sixty-eight (23.1%) patients with clinically large tumors were treated with neoadjuvant therapy prior to surgery. Pathological tumor size and treatment information was not available in two patients. Separately, 22 of the 294 patients were diagnosed with biopsy-confirmed multifocal or multicentric disease.

### **Breast Cancer Type**

Breast cancer type was retrieved from surgical or biopsy pathology reports. The dominant breast cancer type was invasive ductal carcinoma (IDC), followed by invasive mammary carcinoma (IMC, a mixture of invasive ductal and lobular carcinomas), and invasive lobular carcinoma (ILC). Cancer type information was not available for two patient. Another patient was diagnosed with a high-grade neoplasm with neuroendocrine differentiation. Breast cancer type distribution is listed in Table 2.

### **Breast Tumor Location in Relation to Adipose Tissue**

Visual inspection of the enhanced MRI images demonstrated that 291 of 294 patients had invasive breast tumors located at the interface between fibroglandular and adipose (IFFA) tissues, regardless of the tumor size, tumor type, receptor status, or breast density. The remaining three patients had tumors that were too small to be visualized on the enhanced MRI images in the presence of strong background enhancement.

Specifically, invasive breast tumors were identified at the IFFA in patients with unifocal disease, regardless of tumor size, receptor status, type, or breast density (representative images in Figure 1a – f). Moreover, unifocal breast tumors (representative image Figure 2a) were identified surrounded by adipose tissue apart from the main fibroglandular parenchyma (representative image Figure 2b) in nine patients. Each breast tumors was also identified at the IFFA in 22 patients with multifocal or multicentric disease (representative images Figure 3a – 3d). In addition, invasive breast tumor location at the IFFA was independent of the

DCE-MRI image acquisition protocols. Tumor location at the IFFA was also confirmed in all 19 patients whose DCE-MRI images were acquired with fat saturation, with some representative images shown in Figure 4a – 4c. In summary, 100% of the DCE-MRI conspicuous invasive breast tumors in the current study population were observed at the IFFA.

### Adipose Tissue Expansion Pattern

Figure 5 demonstrates the effect of body adiposity on adipose tissue expansion in four invasive breast cancer patients between 31 – 32 years old. Top row shows the increasing thickness of the UAAL of these patients. The center row of Figure 5 demonstrates that, as the thickness of the UAAL increased, subcutaneous adipose tissue expanded inward from the breast periphery, and retromammary adipose tissue expanded outward from the chest wall. The expansion of adipose tissue is accompanied by the concurrent regression of fibroglandular tissue. Eventually, a patient with an 18 mm thick UAAL had almost entirely fatty breasts at age 32. Figure 6 demonstrates the effect of age on adipose tissue expansion in four invasive breast cancer patients with the same thickness of UAAL of 10 mm from age 27 to 69. The center row of Figure 6 demonstrates a similar adipose tissue expansion pattern as that in Figure 5.

Figures 5 and 6 demonstrate that the expansion of adipose tissue and the regression of the fibroglandular tissue, *i.e.*, breast involution, can be mediated by either body adiposity or age. Invasive breast tumors were predominantly observed at the interface between adipose tissue and fibroglandular tissue, where the expansion of adipose tissue and the regression of the fibroglandular tissue occurred concurrently.

### Discussion

Our results demonstrated that invasive breast tumors preferably and predominantly occurred at the IFFA. This finding is in accordance with an earlier histology study of 310 patients, which demonstrated that adipose tissue was present in 79.0% of breast tumor margins<sup>4</sup>. However, breast DCE-MRI images have the advantage of providing a view of the entire tumor and its surroundings noninvasively, without disrupting the native tumor environment. The microscopic histologic study<sup>4</sup>, combined with our macroscopic MRI observation, indicate that adipose tissue plays an indispensable role in breast cancer initiation and progression.

The consistent breast tumor location at the IFFA suggests a common breast cancer etiology, regardless of breast density, tumor receptor status, type, or tumor size. Henson and others had proposed that the rate and the extent of involution may be important factors in breast cancer etiology<sup>14</sup>. Involution results in the loss of glandular tissue by controlled apoptosis of epithelial cells and their replacement by adipose cells through adipocyte differentiation<sup>25</sup>. The degree of complete involution is associated with a reduced risk of breast cancer<sup>17</sup>. We hypothesized that the IFFA is where involution, the expansion of adipose tissue and regression of fibroglandular tissue, happens. Breast carcinoma carcinogenesis is a multi-phase malignant transformation of the normal breast epithelial cells<sup>26</sup>, from hyperplasia, to atypia, to in situ malignancy, and to invasive malignancy. We hypothesized that aberrations

in involution may contribute directly to the malignant transformation of normal breast cells, in addition to the reported benign breast conditions<sup>27</sup>. Furthermore, both excessive adiposity<sup>10, 28</sup> and post-lactation involution<sup>18, 29, 30</sup> are associated with elevated pro-inflammation mediator expression, which is conducive to tumor formation. We hypothesized that aberration in involution produces the breast cancer seeds that grow in the fertile adipose soil at the IFFA.

Breast cancer rates increase with age, as breast tissue undergoes atrophy due to lobular involution<sup>14</sup>. Incidentally, fewer pregnancy-related breast cancers are diagnosed during pregnancy<sup>31</sup> when extensive breast glandular cell differentiation and growth occurred<sup>29</sup>. More pregnancy-associated breast cancers were diagnosed 7 to 24 months after the birth<sup>31</sup>, during which mammary involution may dominate. Similarly, breast cancer risk is low during puberty, during which dramatic mammary gland growth occurs. Collectively, this suggests a strong link between involution and breast cancer. Unfortunately, our understanding of breast involution, particularly the age-related lobular involution process, is very limited.

Our discovery demonstrates the potential importance of adipose tissue in the development of breast cancer. More research is needed to understand the breast involution process and the cross-talk mechanism between breast epithelial cells and adipocytes, which may enhance the malignant transformation of normal breast cells. A greater understanding of these processes may enable the development of new breast cancer prevention, detection, and treatment approaches.

## Acknowledgments

We thank Dr. Venu Raman for helpful discussions. We are grateful to Ms. Mary McAllister for editorial help with this manuscript. This study has received funding by the National Cancer Institutes CA154738.

## References

1. Elenbaas B, Spirio L, Koerner F, et al. Human breast cancer cells generated by oncogenic transformation of primary mammary epithelial cells. *Genes. Dev.* 2001; 15:50–65. [PubMed: 11156605]
2. Quail DF, Joyce JA. Microenvironmental regulation of tumor progression and metastasis. *Nat. Med.* 2013; 19:1423–1437. [PubMed: 24202395]
3. Tan J, Buache E, Chenard MP, Dali-Youcef N, Rio MC. Adipocyte is a non-trivial, dynamic partner of breast cancer cells. *Int J Dev Biol.* 2011; 55:851–859. [PubMed: 21948738]
4. Yamaguchi J, Ohtani H, Nakamura K, Shimokawa I, Kanematsu T. Prognostic impact of marginal adipose tissue invasion in ductal carcinoma of the breast. *Am J Clin Pathol.* 2008; 130:382–388. [PubMed: 18701411]
5. Dirat B, Bochet L, Dabek M, et al. Cancer-associated adipocytes exhibit an activated phenotype and contribute to breast cancer invasion. *Cancer. Res.* 2011; 71:2455–2465. [PubMed: 21459803]
6. Liu E, Samad F, Mueller BM. Local adipocytes enable estrogen-dependent breast cancer growth: Role of leptin and aromatase. *Adipocyte.* 2013; 2:165–169. [PubMed: 23991363]
7. Place AE, Jin Huh S, Polyak K. The microenvironment in breast cancer progression: biology and implications for treatment. *Breast Cancer. Res.* 2011; 13:227. [PubMed: 22078026]
8. Calle EE, Kaaks R. Overweight, obesity and cancer: epidemiological evidence and proposed mechanisms. *Nature reviews. Cancer.* 2004; 4:579–591. [PubMed: 15286738]
9. Byers T, Sedjo RL. Body fatness as a cause of cancer: epidemiologic clues to biologic mechanisms. *Endocr Relat Cancer.* 2015; 22:R125–R134. [PubMed: 25870250]

10. Hefetz-Sela S, Scherer PE. Adipocytes: impact on tumor growth and potential sites for therapeutic intervention. *Pharmacol Ther.* 2013; 138:197–210. [PubMed: 23353703]
11. Park J, Morley TS, Kim M, Clegg DJ, Scherer PE. Obesity and cancer--mechanisms underlying tumour progression and recurrence. *Nat Rev Endocrinol.* 2014; 10:455–465. [PubMed: 24935119]
12. Park J, Euhus DM, Scherer PE. Paracrine and endocrine effects of adipose tissue on cancer development and progression. *Endocr. Rev.* 2011; 32:550–570. [PubMed: 21642230]
13. Iyengar NM, Hudis CA, Dannenberg AJ. Obesity and cancer: local and systemic mechanisms. *Annu. Rev Med.* 2015; 66:297–309. [PubMed: 25587653]
14. Henson DE, Tarone RE. On the possible role of involution in the natural history of breast cancer. *Cancer.* 1993; 71:2154–2156. [PubMed: 8443765]
15. Ginsburg OM, Martin LJ, Boyd NF. Mammographic density, lobular involution, and risk of breast cancer. *Br J Cancer.* 2008; 99:1369–1374. [PubMed: 18781174]
16. Ghosh K, Hartmann LC, Reynolds C, et al. Association between mammographic density and age-related lobular involution of the breast. *Journal of clinical oncology : official journal of the American Society of Clinical Oncology.* 2010; 28:2207–2212. [PubMed: 20351335]
17. Milanese TR, Hartmann LC, Sellers TA, et al. Age-related lobular involution and risk of breast cancer. *J Natl Cancer Inst.* 2006; 98:1600–1607. [PubMed: 17105983]
18. Schedin P. Pregnancy-associated breast cancer and metastasis. *Nature reviews. Cancer.* 2006; 6:281–291. [PubMed: 16557280]
19. Schneider CA, Rasband WS, Eliceiri KW. NIH Image to ImageJ: 25 years of image analysis. *Nat Methods.* 2012; 9:671–675. [PubMed: 22930834]
20. Schindelin J, Arganda-Carreras I, Frise E, et al. Fiji: an open-source platform for biological-image analysis. *Nat Methods.* 2012; 9:676–682. [PubMed: 22743772]
21. Zhu W, Huang P, Macura KJ, Artemov D. Association between breast cancer, breast density, and body adiposity evaluated by MRI. *European radiology.* 2015 Epub ahead of print.
22. Saslow D, Boetes C, Burke W, et al. American Cancer Society guidelines for breast screening with MRI as an adjunct to mammography. *CA Cancer J Clin.* 2007; 57:75–89. [PubMed: 17392385]
23. Hammond ME, Hayes DF, Dowsett M, et al. American Society of Clinical Oncology/College of American Pathologists guideline recommendations for immunohistochemical testing of estrogen and progesterone receptors in breast cancer (unabridged version). *Archives of pathology & laboratory medicine.* 2010; 134:e48–e72. [PubMed: 20586616]
24. AJCC (American Joint Committee on Cancer). *Cancer Staging Manual.* 7th. New York: Springer-Verlag; 2010.
25. Watson CJ. Involution: apoptosis and tissue remodelling that convert the mammary gland from milk factory to a quiescent organ. *Breast Cancer. Res.* 2006; 8:203. [PubMed: 16677411]
26. Beckmann MW, Niederacher D, Schnurch HG, Gusterson BA, Bender HG. Multistep carcinogenesis of breast cancer and tumour heterogeneity. *J Mol Med (Berl).* 1997; 75:429–439. [PubMed: 9231883]
27. Hughes LE, Mansel RE, Webster DJ. Aberrations of normal development and involution (ANDI): a new perspective on pathogenesis and nomenclature of benign breast disorders. *Lancet.* 1987; 2:1316–1319. [PubMed: 2890912]
28. Howe LR, Subbaramaiah K, Hudis CA, Dannenberg AJ. Molecular pathways: adipose inflammation as a mediator of obesity-associated cancer. *Clinical cancer research : an official journal of the American Association for Cancer Research.* 2013; 19:6074–6083. [PubMed: 23958744]
29. Radisky DC, Hartmann LC. Mammary involution and breast cancer risk: transgenic models and clinical studies. *J Mammary Gland Biol Neoplasia.* 2009; 14:181–191. [PubMed: 19404726]
30. McDaniel SM, Rumer KK, Biroc SL, et al. Remodeling of the mammary microenvironment after lactation promotes breast tumor cell metastasis. *Am J Pathol.* 2006; 168:608–620. [PubMed: 16436674]
31. Andersson TM, Johansson AL, Hsieh CC, Cnattingius S, Lambe M. Increasing incidence of pregnancy-associated breast cancer in Sweden. *Obstet Gynecol.* 2009; 114:568–572. [PubMed: 19701036]



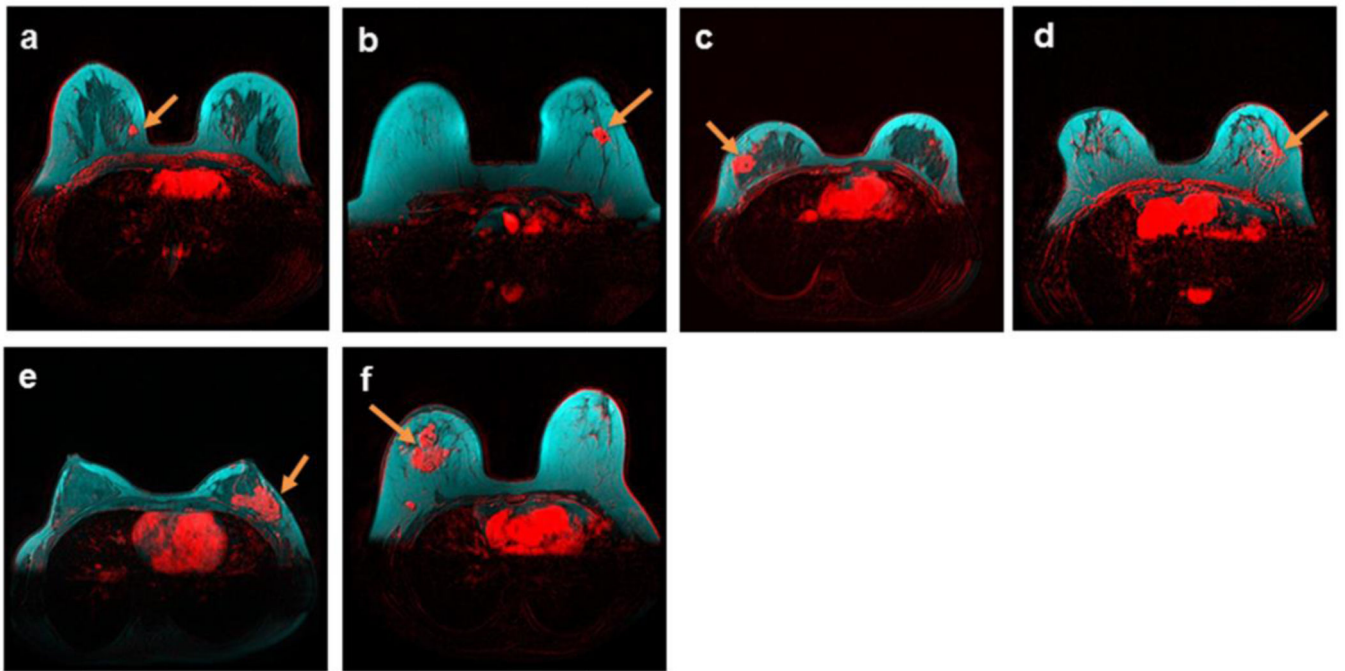


**Figure 1.**

Unifocal breast tumors (red) of different sizes, receptor status and types at the fibroglandular (dark) and adipose (cyan) tissue interface, demonstrated by breast DCE-MRI enhancement at plateau, and overlaid on T<sub>1</sub>-weighted pre-contrast images without fat saturation. Enhanced tumors are indicated by arrows. a) A 41-year-old patient with a breast density of 39.8%, and a stage 1 estrogen receptor-positive IDC tumor; b) a 44-year-old patient with a breast density of 6.6%, and a stage 1 estrogen receptor-positive IMC tumor; c) a 35-year-old patient with a breast density of 30.9%, and a stage 2 triple-negative IDC tumor; d) an 80-year-old patient with a breast density of 9%, and a stage 2 estrogen- and HER-2 receptor-positive ILC tumor; e) a 44-year-old patient with a breast density of 56.3%, and a stage 3 estrogen receptor-positive IDC tumor; and f) a 46-year-old patient with a breast density of 6.5%, and an estrogen receptor-positive IDC tumor > 7 cm.

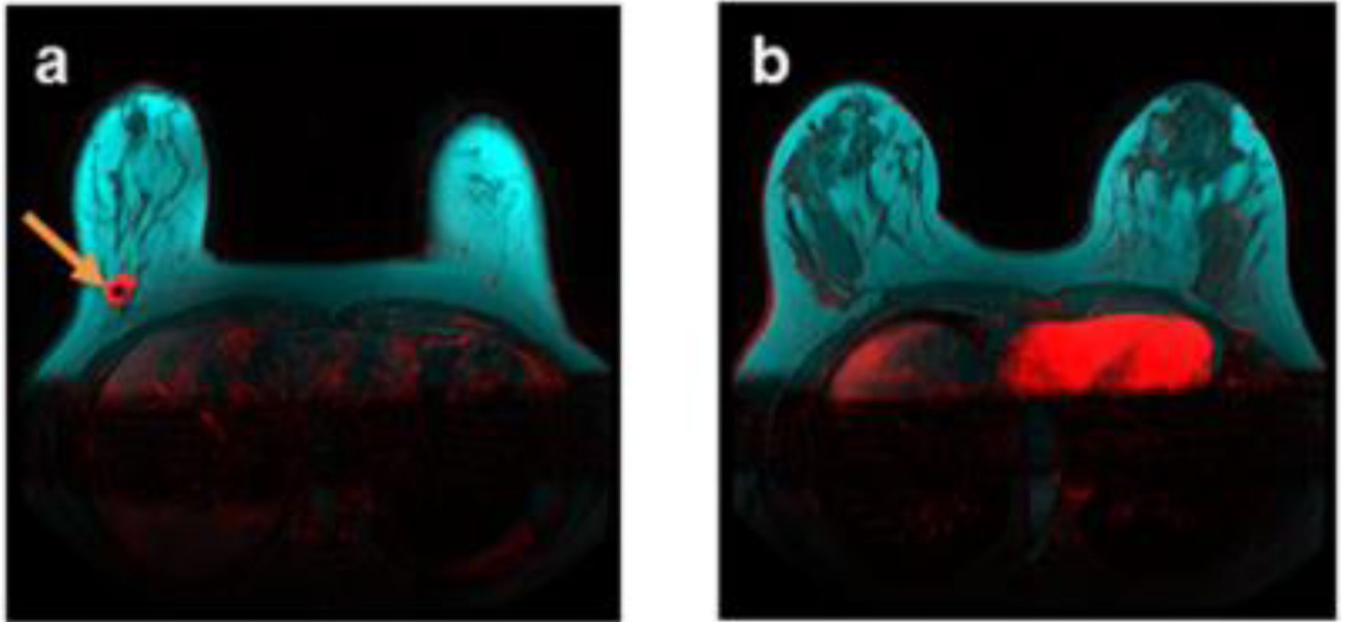


**Figure 2.** Isolated unifocal breast tumor (red), demonstrated by breast DCE-MRI enhancement at plateau and overlaid on T<sub>1</sub>-weighted pre-contrast images without fat saturation, surrounded by adipose tissue (cyan) apart from the main breast fibroglandular parenchyma (dark). Enhanced tumor is indicated by arrows. a) An estrogen receptor-positive stage 1 IDC tumor at the fibroglandular and adipose interface in a 61-year-old patient with a breast density of 21.6%; apart from the b) main fibroglandular parenchyma of the same patient.

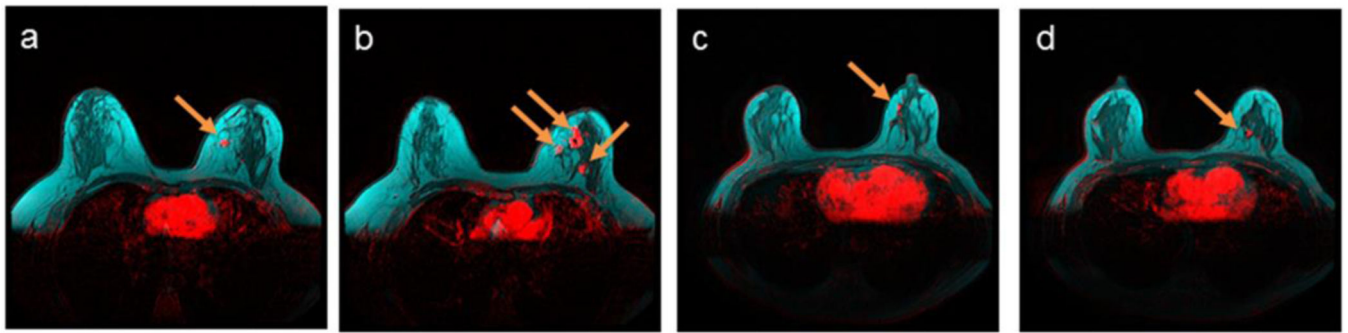


**Figure 3.** Multifocal breast tumors (red) at the fibroglandular (dark) and adipose (cyan) tissue interface, demonstrated by breast DCE-MRI enhancement at plateau, and overlaid on  $T_1$ -weighted pre-contrast images without fat saturation. Enhanced tumors are indicated by arrows. a) and b) Stage 2 multifocal estrogen receptor-positive IDC tumors in a 38-year-old patient with a breast density of 21.5%; c) and d) stage 1 estrogen receptor-positive multifocal ILC tumors in a 50-year-old patient with a breast density of 32.1%.

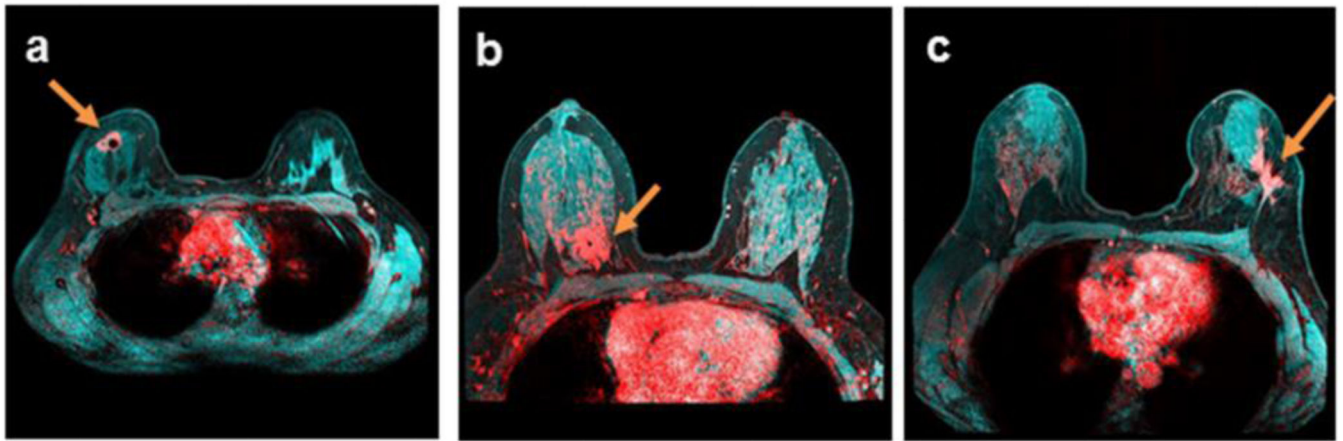


**Figure 4.**

Breast tumors (red) at the fibroglandular (cyan) and adipose (dark) tissue interface, demonstrated by breast DCE-MRI enhancement at plateau, and overlaid on T<sub>1</sub>-weighted pre-contrast images with fat saturation. Enhanced tumors are indicated by arrows. a) An estrogen receptor-positive IDC tumor in a 35-year-old patient with a breast density of 37.0%; b) an estrogen receptor- and HER-2 receptor-positive IDC tumor in a 51-year-old patient with a breast density of 43.6%; c) estrogen receptor-positive multicentric IDC tumors in a 44-year-old patient with a breast density of 24.6%

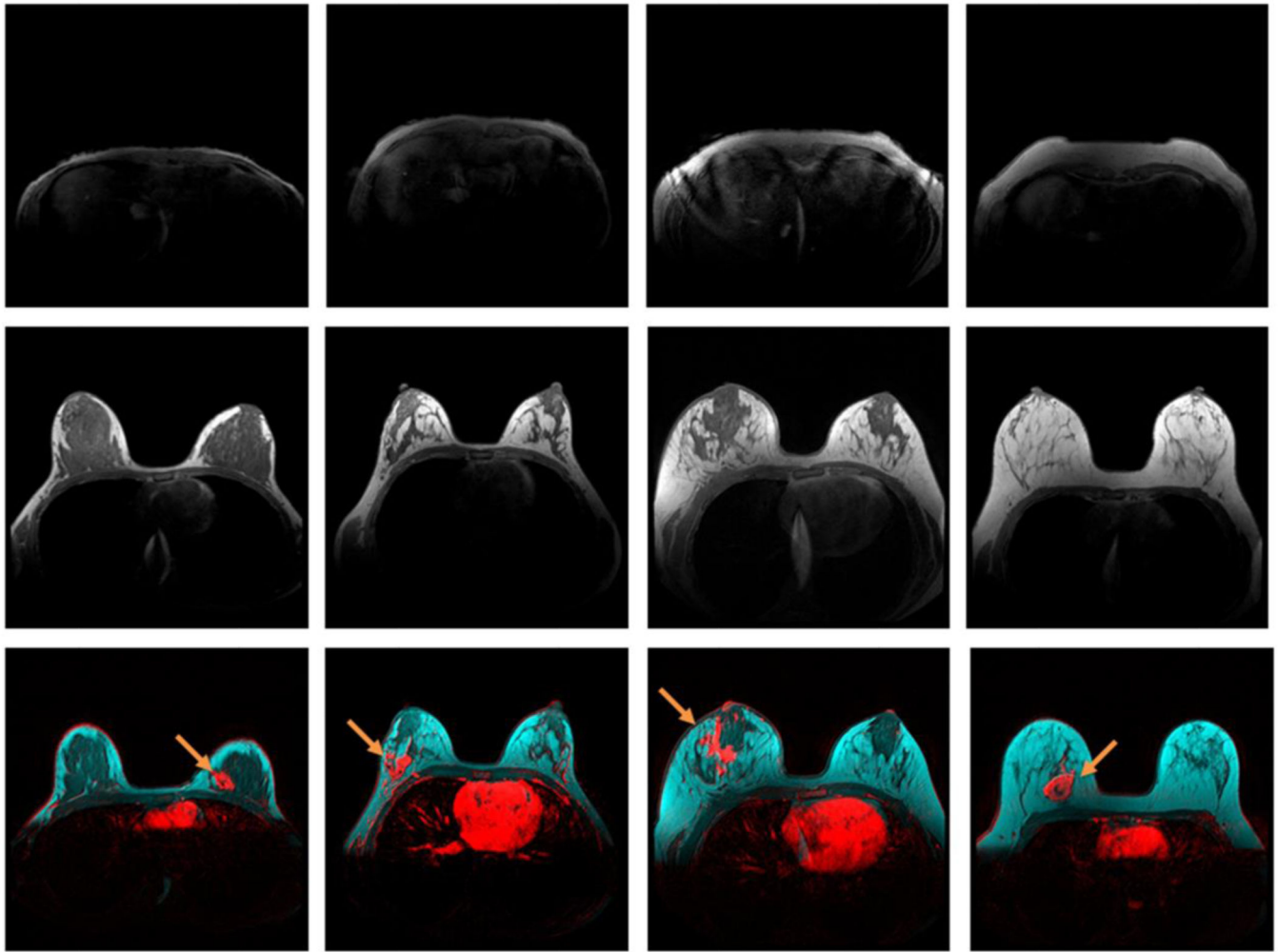


**Figure 5.**

Effect of body adiposity on breast adipose tissue expansion in women 31 – 32 years old. Top row: UAAL on T<sub>1</sub>-weighted pre-contrast images; center row: central breast on T<sub>1</sub>-weighted pre-contrast images; and bottom row: breast tumors (red) at the fibroglandular (dark) and adipose (cyan) tissue interface, demonstrated by breast DCE-MRI enhancement at plateau, and overlaid on T<sub>1</sub>-weighted pre-contrast images without fat saturation. Enhanced tumors are indicated by arrows. Images from left to right: a 32-year-old patient with a UAAL thickness of 2 mm, a breast density of 68.0%, and an estrogen receptor-positive IMC tumor; a 32-year-old patient with a UAAL thickness of 5 mm, a breast density of 24.5%, and an estrogen receptor-positive IMC tumor; a 31-year-old patient with a UAAL thickness of 13 mm, a breast density of 22.4%, and a triple-negative IDC tumor; and a 32-year-old patient with a UAAL thickness of 18 mm, a breast density of 5.2%, and an estrogen receptor-positive IDC tumor.

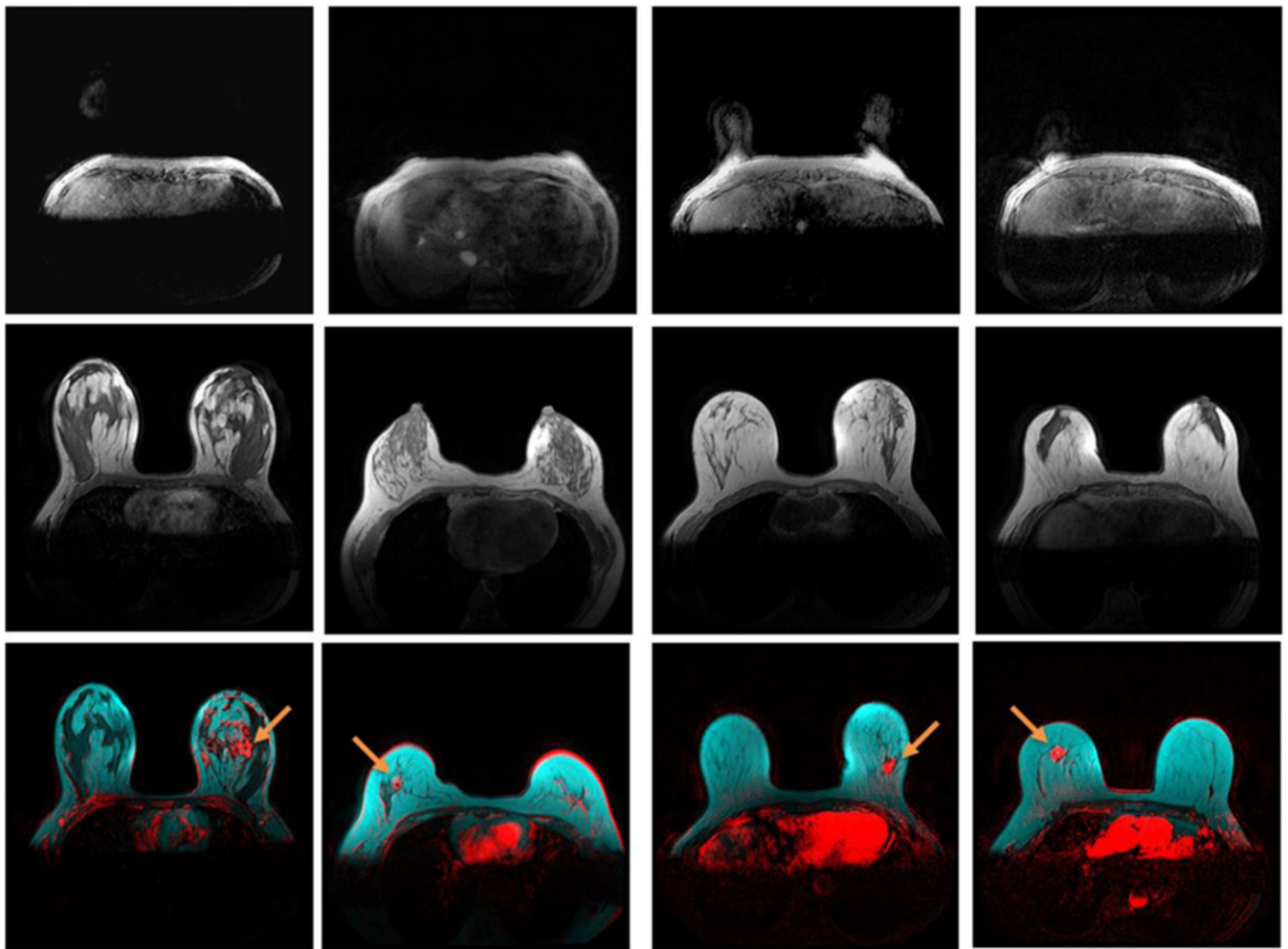


**Figure 6.**

Effect of age on breast adipose tissue expansion in women with a fixed UAAL thickness of 10 mm. Top row: UAAL on T<sub>1</sub>-weighted pre-contrast images; center row: central breast on T<sub>1</sub>-weighted pre-contrast images; and bottom row: breast tumors (red) at the fibroglandular (dark) and adipose (cyan) tissue interface, demonstrated by breast DCE-MRI enhancement at plateau, and overlaid on T<sub>1</sub>-weighted pre-contrast images without fat saturation. Enhanced tumors are indicated by arrows. Images from left to right: a 27-year-old patient with a breast density of 37.4% and an estrogen- and HER-2 receptor-positive IDC tumor; a 36-year-old patient with a breast density of 24.0% and an estrogen receptor-positive IMC tumor; a 47-year-old patient with a breast density of 9.5% and an estrogen receptor-positive IDC with medullary features tumor; and a 69-year-old patient with a breast density of 9.6% and an estrogen receptor-positive ILC tumor.

**Table 1**

Age, the thickness of the UAAL, and breast density distribution

Age groups (year)	20 – 30	31 – 40	41 – 50	51 – 60	61 – 70	> 71
Patient counts, percentage %	9, 3	41, 14	77, 26	100, 34	47, 16	20, 7
Mean, median thickness of the UAAL (mm)	5.0, 3.0	10.7, 10.0	12.9, 12.0	17.0, 16.5	17.8, 12.5	16.3, 12.9
Mean, median breast density (%)	49.2, 49.6	30.2, 24.5	23.2, 19.3	15.6, 11.3	12.5, 9.6	12.9, 8.7

**Table 2**

## Breast Cancer Type Distribution

	<b>IDC</b>	<b>IMC</b>	<b>ILC</b>	<b>Other</b>
Patient counts, percentage %	205, 70	52, 18	31, 11	5, 2

IDC: invasive ductal carcinoma

IMC: invasive mammary carcinoma

ILC: invasive lobular carcinoma

Other: 2 infiltrating ductal carcinoma with mucinous features, 1 infiltrating ductal carcinoma with medullary features, 1 had a high grade neoplasm with neuroendocrine differentiation, and breast cancer type information was not available in 1 other patients.